Endocrinology, 2022, **163**, 1–12
https://doi.org/10.1210/endocr/bqac001
Advance access publication 06 January 2022
Research Article

Comprehensive Sex Steroid Profiling in Multiple Tissues Reveals Novel Insights in Sex Steroid Distribution in Male Mice

Hannah Colldén,[1,2,*] Maria E Nilsson,[1,3,*] Anna-Karin Norlén,[3] Andreas Landin,[2] Sara H Windahl,[4] Jianyao Wu,[1] Karin L Gustafsson,[1] Matti Poutanen,[1,5] Henrik Ryberg,[3] Liesbeth Vandenput,[1,*] and Claes Ohlsson[1,2,*]

[1]Sahlgrenska Osteoporosis Centre, Centre for Bone and Arthritis Research, Department of Internal Medicine and Clinical Nutrition, Institute of Medicine, Sahlgrenska Academy, University of Gothenburg, SE-413 45 Gothenburg, Sweden
[2]Department of Drug Treatment, Sahlgrenska University Hospital, Region Västra Götaland, SE-413 45 Gothenburg, Sweden
[3]Department of Clinical Chemistry, Sahlgrenska University Hospital, Region Västra Götaland, Gothenburg SE-413 45, Sweden
[4]Department of Laboratory Medicine, Division of Pathology, Karolinska Institute, Huddinge, Sweden
[5]Department of Physiology, Institute of Biomedicine and Turku Center for Disease Modeling, University of Turku, Turku FI-20014, Finland

Correspondence: Claes Ohlsson, MD, PhD, Sahlgrenska Osteoporosis Centre, Centre for Bone and Arthritis Research, Department of Internal Medicine and Clinical Nutrition, Institute of Medicine, Sahlgrenska Academy, University of Gothenburg, Vita Stråket 11, SE-41345 Göteborg, Sweden. Email: Claes.Ohlsson@medic.gu.se.
*These authors contributed equally

Abstract

A comprehensive atlas of sex steroid distribution in multiple tissues is currently lacking, and how circulating and tissue sex steroid levels correlate remains unknown. Here, we adapted and validated a gas chromatography tandem mass spectrometry method for simultaneous measurement of testosterone (T), dihydrotestosterone (DHT), androstenedione, progesterone (Prog), estradiol, and estrone in mouse tissues. We then mapped the sex steroid pattern in 10 different endocrine, reproductive, and major body compartment tissues and serum of gonadal intact and orchiectomized (ORX) male mice. In gonadal intact males, high levels of DHT were observed in reproductive tissues, but also in white adipose tissue (WAT). A major part of the total body reservoir of androgens (T and DHT) and Prog was found in WAT. Serum levels of androgens and Prog were strongly correlated with corresponding levels in the brain while only modestly correlated with corresponding levels in WAT. After orchiectomy, the levels of the active androgens T and DHT decreased markedly while Prog levels in male reproductive tissues increased slightly. In ORX mice, Prog was by far the most abundant sex steroid, and, again, WAT constituted the major reservoir of Prog in the body. In conclusion, we present a comprehensive atlas of tissue and serum concentrations of sex hormones in male mice, revealing novel insights in sex steroid distribution. Brain sex steroid levels are well reflected by serum levels and WAT constitutes a large reservoir of sex steroids in male mice. In addition, Prog is the most abundant sex hormone in ORX mice.

Key Words: gas chromatography mass spectrometry, mice, tissue, androgens, progesterone, gonadal steroid hormones

Abbreviations: A-dione, androstenedione; BW, body weight; CYP17A1, 17α-dehydroxylase; DHT, dihydrotestosterone; E1, estrone; E2, estradiol; GC-MS/MS, gas chromatography–tandem mass spectrometry; LLOQ, lower limit of quantification; MS, mass spectrometry; ORX, orchiectomized; Prog, progesterone; SHBG, sex hormone–binding globulin; SPE, solid phase extraction; SS, sex steroid; T, testosterone; WAT, white adipose tissue.

Sex steroids (SSs) are vital in development and reproductive function and have effects in a wide variety of tissues in males. SSs are produced from a cholesterol backbone, and in males the testes and adrenal glands produce both precursors and active SSs, which can then be further metabolized in peripheral tissues (1). The weak androgen androstenedione (A-dione) can be produced either by 3β-hydroxysteroid dehydrogenase activity from dehydroepiandrosterone or by 17α-dehydroxylase (CYP17A1) in 2 steps from progesterone (Prog). A-dione can then be activated by HSD17B enzymes into the major circulating androgen testosterone (T), which can either be converted by 5α-reductases (SRD5A1 or SRD5A2) into the most potent androgen dihydrotestosterone (DHT) or aromatized by aromatase (CYP19A1) into the most potent estrogen estradiol (E2). E2 can also be produced via aromatization of A-dione to estrone (E1), which is then further metabolized to E2 by HSD17Bs (2, 3). DHT can also be produced via the so-called backdoor pathway through several enzymatic steps from Prog bypassing T as an intermediate (4) (Fig. 1).

In addition to the production of SSs in the testes and adrenals in males, controlled via the hypothalamic–pituitary–gonadal axis and hypothalamic–pituitary–adrenal axis, respectively, SSs can also be produced and metabolized in several other tissues that express all required enzymes, for example in the brain and the prostate (5, 6). As such, circulating SS levels may not always reflect SS levels in target tissues. In addition to the systemic supply via the blood circulation, local synthesis and metabolism of SSs in target tissues plays a

Received: 9 November 2021. **Editorial Decision:** 30 December 2021. **Corrected and Typeset:** 1 February 2022

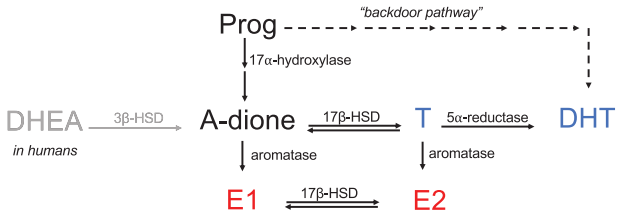

Figure 1. Schematic presentation of the sex steroids analyzed and their metabolic relationships. Active androgens are indicated in blue, active estrogens in red. DHEA, dehydroepiandrosterone; Prog, progesterone; A-dione, androstenedione; T, testosterone; DHT, dihydrotestosterone; E1, estrone; E2, estradiol; HSD, hydroxysteroid dehydrogenase.

key role in several SS responses, and is involved in the pathogenesis of various diseases such as prostate and breast cancer, metabolic diseases, and diseases of the central nervous system (5, 7-9). For example, CYP17A1 inhibitors are used to prevent local androgen production in the tumors of patients with castration-resistant prostate cancer, and aromatase inhibitors are used to prevent local E2 synthesis in postmenopausal women with estrogen receptor–positive breast cancer (8, 9).

The mouse is a common model of human diseases due to its versatility and relatively low cost. However, due to the lack of sex hormone–binding globulin (SHBG) in mice (10), resulting in very low levels of circulating SSs, sensitive and specific methods are needed to accurately quantify SSs in mouse serum and tissues (11-13). The gold standard method for quantification of SSs is mass spectrometry (MS), with the advantage of analyzing multiple analytes in a single run (14-16). Previous studies have quantified various SS levels in selected tissues of both humans and animal models (11, 17-23). However, to the best of our knowledge, a comprehensive atlas of SS distribution in multiple tissues analyzed simultaneously by a validated MS-based method is currently lacking. Also, it remains largely unknown to what extent circulating levels of SSs correlate with tissue levels of SSs in male mice.

We here adapted and validated a gas chromatography–tandem MS (GC-MS/MS) method for the simultaneous measurement of a broad panel of SSs in several different types of tissues in mice. This method was used to map the SS pattern in the circulation and 10 different endocrine, reproductive, and major body compartment tissues, revealing novel insights in SS distribution in gonadal intact and orchiectomized (ORX) male mice.

Materials and Methods

Animals and Procedures

Male C57BL/6J mice (Taconic, Ry, Denmark) were kept in individually ventilated cages in a standard animal facility with controlled temperature (23°C) and 12-hour light/dark cycle and ad libitum access to standard chow pellets and tap water. At 8-10 weeks of age they were subjected to orchiectomy or sham surgery (Sham). The number of mice in each group was 10. Surgery was performed under anesthesia with isoflurane (Baxter Medical AB, Kista, Sweden). Postoperative analgesia was Rimadyl (Orion Pharma AB, Animal Health, Sollentuna, Sweden). Four weeks later the mice were anesthetized with Ketanest and Dormitor (Pfizer/Orion Pharma), bled, and euthanized by cervical dislocation. Blood was allowed to coagulate at room temperature for 30 minutes and then centrifuged to collect the serum. Liver, gonadal fat, brain cortex, adrenals, m. quadriceps, m. levator ani, humerus diaphyseal cortical bone, testicles, seminal vesicles, and prostate were collected and snap frozen. In ORX males, for technical reasons prostate samples were only available from 3 out of 10 animals. The experiment was conducted in accordance with all relevant legislation and was approved by the ethics committee of the University of Gothenburg.

Sample Preparation

Frozen tissues were thawed on ice. For small organs, the whole organ was used for sample preparation while for larger organs/tissues we aimed to use 125 mg for sample preparation. The tissue was weighed and placed in a 2-mL screw-top Eppendorf tube with 450 µL of phosphate-buffered saline. The samples were homogenized by shaking with a 5-mm steel bead in a Tissuelyzer II for 5 minutes. Serum samples were measured volumetrically by pipetting and adjusted to a volume of 450 µL with deionized water.

Sample Extraction and GC-MS/MS Analysis

SSs were extracted, derivatized, and measured as described previously (12, 22). Briefly, after addition of isotope-labeled standards, SSs were first extracted by liquid–liquid extraction with 1-chlorobutane, followed by solid phase extraction (SPE) using Silica SPE columns (SupraClean, Perkin Elmer, Waltham, MA, USA) that were washed 2 times with ethylacetate–pentane–heptane (10:45:45 [vol:vol]). For liver and adipose tissue samples, 3 washing steps instead of the regular 2 were used to reach an optimal performance in the GC-MS/MS assay. Then, derivatization was performed in 2 steps: oximation with pentafluorobenzylhydroxylamine hydrochloride and esterification with pentafluorobenzoyl chloride. Finally, E2, E1, Prog, DHT, T, and A-dione were separated using gas chromatography and detected simultaneously with electron capture negative chemical ionization by an Agilent 7000 triple quadrupole mass spectrometer (Agilent, Santa Clara, CA, USA) operating in multiple reaction monitoring mode with ammonia as reagent gas. All peaks were integrated using the MassHunter quantitative analysis workstation software from Agilent. Representative examples of extracted ion chromatograms of the analytes in bone and mass transitions used are shown elsewhere (Figure 1 (24)).

Validation

Detailed assay validation was performed in 4 mouse tissues with very different matrix compositions: white adipose tissue (WAT; gonadal fat, high fat content), muscle (m. quadriceps, low fat content), bone (cortical bone, calcified matrix), and liver (metabolite-rich matrix). Tissue samples with low SS content (from gonadectomized mice) were spiked with natural or stable isotope-labeled SSs (depending on the baseline concentration of the analyte in question in the assayed tissue). The lower limit of quantification (LLOQ) was defined as the lowest peak having a signal at >3 times the noise level, that was reproducible with a coefficient of variation of less than 20% and an accuracy of 80% to 120%. Seven different levels in the lower concentration range of each SS were evaluated to determine the LLOQ in each tissue. Precision was calculated as the intra-assay coefficient of variation between the samples on the same concentration level. Accuracy was calculated as (measured level – baseline level)/spiked level × 100%. Precision and accuracy were determined using the mean of 3

to 4 samples on each concentration level. Extraction recovery was evaluated in muscle and WAT with isotope-labeled steroids and calculated as the ratio between samples spiked before the liquid–liquid extraction and after SPE column extraction. Linearity was determined using a spiked sample at the same concentration as the highest point on the standard curve that was serially diluted before extraction and R^2 was calculated. The high sensitivity GC-MS/MS method used for the quantification of SSs in mouse serum has been described previously (12) with the only modification that the LLOQ for DHT was 1.4 pg/mL in the present study.

Calculations/Statistics

SS levels below the LLOQ were set to the LLOQ. SS levels are only reported for groups in which at least half of the measurements were >LLOQ, otherwise they are denoted not detected. One milliliter of serum was considered equivalent to 1 gram of tissue. We used a simplified model to estimate the amounts of all determined SS levels in different compartments of the mouse body. The total pool of each SS was calculated as the sum of the SS amounts of every tissue, calculated as tissue weight × measured concentration. The model was based on individually measured tissue weights (prostate, m. levator ani, seminal vesicles), fixed approximated tissue weights (adrenals, testicles), and body weights (BWs) at sacrifice. The following assumptions were made: the concentration in m. quadriceps was used to approximate the concentration in lean mass (65% of BW), the concentration in the large gonadal fat depot to approximate the concentration in adipose tissue (20% of BW), the concentration in brain cortex to approximate the concentration in brain tissue (2.5% of BW), and the concentration in cortical bone to approximate the concentration in the skeleton (2% of BW). Liver weight was calculated as 4.5% of BW.

SS concentrations are presented as median and interquartile range (IQR) unless stated otherwise. SS levels in the Sham and ORX groups were compared using the Mann–Whitney U-test. Tissue levels of SSs were compared with serum levels using paired Wilcoxon rank tests, corrected for 10 multiple comparisons using the Holm–Sidak method. Spearman rank-order correlations were used to test the correlations between SS levels in serum and different tissues. GraphPad Prism 9 (GraphPad, San Diego, CA, USA) and SPSS 27 (IBM, Armonk, NY, USA) were used for statistical analyses. $P < .05$ was considered statistically significant.

Results

Evaluation of Assay Performance

We evaluated the performance of the assay using 4 tissues with very different matrix compositions: *WAT* with high fat content, *muscle* with low fat content, *bone* that is a calcified tissue, and *liver* that is rich in metabolites and thus a complex matrix to analyze. The method showed high sensitivity for all SSs in all evaluated tissues with LLOQs of 2 to 2.8 pg/g for E2, 2 to 4 pg/g for E1, 20 to 40 pg/g for T, 4 to 8 pg/g for DHT, 75 pg/g for Prog, and 7.5 pg/g for A-dione (Table 1). The precision was good, with interassay coefficients of variation below 20% for all analytes in all tissues both at high and low concentration (Table 2). The accuracy for the different

Table 1. Sensitivity of assay as lower limit of quantification (LLOQ) in different tissues

	Estradiol	Estrone	Testosterone	DHT	Progesterone	Androstenedione
Muscle (pg/g)	2.0	2.0	20	8.0	75	7.5
Liver (pg/g)	2.8	4.0	40	4.0	75	7.5
WAT (pg/g)	2.0	2.0	40	4.0	75	7.5
Bone (pg/g)	2.0	2.0	20	8.0	75	7.5

Abbreviations: WAT, white adipose tissue; DHT, dihydrotestosterone.

Table 2. Precision of assay as interassay coefficient of variation in different tissues

	Estradiol	Estrone	Testosterone	DHT	Progesterone	Androstenedione
Muscle						
QC-low	10.5% (8.7)	11.5% (10.0)	7.5% (139)	18.9% (28.1)	0.5% (250)	4.2% (104)
QC-high	4.0% (83.2)	2.4% (79.2)	1.6% (1050)	6.0% (215)	0.3% (1980)	1.0% (479)
Liver						
QC-low	5.1% (58.1)	5.3% (68.4)	2.0% (97.0)	5.0% (16.6)	1.3% (195)	4.5% (48.6)
QC-high	2.6% (453)	2.1% (485)	0.2% (5570)	3.5% (1150)	0.4% (11000)	0.5% (2780)
WAT						
QC-low	8.0% (7.8)	2.8% (7.9)	6.1% (96.4)	4.2% (20.8)	1.5% (169)	1.0% (47.7)
QC-high	3.1% (60.8)	2.1% (59.2)	2.0% (739)	4.0% (152)	0.7% (1430)	1.0% (367)
Bone						
QC-low	7.0% (2.0)	1.0% (2.0)	8.9% (20)	8.7% (8.0)	1.2% (75)	6.2% (75)
QC-high	2.1% (100)	2.3% (100)	3.6% (1000)	5.8% (200)	2.4% (3750)	0.2% (375)

Values within brackets are the concentration for the QC in pg/g.
Abbreviations: WAT, white adipose tissue; DHT, dihydrotestosterone; QC-low, quality control sample with low concentration; QC-high, quality control sample with high concentration.

Table 3. Accuracy in mouse muscle

	Baseline	Spiked	Measured	Accuracy
	(pg/g)	(pg/g)	(pg/g)	(%)
Estradiol				
Low	3.4	10.2	12.1	85
High	3.4	81.5	86.6	102
Estrone				
Low	0.0	10.2	10.1	99
High	0.0	81.5	79.2	97
Testosterone				
Low	26.6	127	166	109
High	26.6	1019	1076	103
Dihydrotestosterone				
Low	0.0	25.5	28.1	110
High	0.0	204	215	106
Progesterone				
Low	317	255	567	98
High	317	2038	2298	97
Androstenedione				
Low	0.0	127	104	82
High	0.0	509	479	94

Accuracy was calculated as (measured level – baseline level)/spiked level × 100%. Sample size: 125 mg.

Table 4. Accuracy in mouse liver

	Baseline	Spiked	Measured	Accuracy
	pg/g	pg/g	pg/g	(%)
Estradiol				
Low	0.0	4.0	4.3	107
High	0.0	10.0	9.9	99
Estrone				
Low	0.0	4.00	3.97	99
High	0.0	10.0	9.4	94
Testosterone				
Low	54.1	90.0	151	108
High	54.1	5400	5625	103
Dihydrotestosterone				
Low	28.6	18.0	45.4	93
High	28.6	1080	1174	106
Progesterone				
Low	139.0	180	334	109
High	139.0	10800	11140	102
Androstenedione				
Low	7.5	45.0	55.9	108
High	7.5	2700	2789	103

Accuracy was calculated as (measured level – baseline level)/spiked level × 100%. Sample size 125 mg.

Table 5. Accuracy in mouse gonadal fat

	Baseline	Spiked	Measured	Accuracy
	(pg/g)	(pg/g)	(pg/g)	(%)
Estradiol				
Low	0.0	7.2	7.8	108
High	0.0	57.6	60.8	106
Estrone				
Low	0.0	7.2	7.9	109
High	0.0	57.6	59.2	103
Testosterone				
Low	17.2	90.0	113	107
High	17.2	720	756	103
Dihydrotestosterone				
Low	13.1	18.0	33.9	115
High	13.1	144	165	106
Progesterone				
Low	3799	180	3968	94
High	3799	1440	5226	99
Androstenedione				
Low	59.9	45.0	108	106
High	59.9	360	427	102

Accuracy was calculated as (measured level – baseline level)/spiked level × 100%. Sample size 125 mg.

analytes was 82% to 110% in muscle, 93% to 109% in liver, 94% to 115% in WAT, and 83% to 119% in cortical bone (Tables 3-6). The extraction recoveries during the preparation of samples were found to be above 80% for all steroids in muscle and WAT, except for E1 and E2 in muscle (66% and 69%, respectively) and T in WAT (62%). A slightly reduced extraction recovery does not influence the absolute quantification of the analytes since $^{13}C_3$-labeled internal standards for all analyzed steroids are added to every sample before the initiation of the extraction. Linearity was excellent ($R^2 > 0.99$) for all analytes in all matrices (Figures 2-5 (24)).

SS Distribution in Serum and Tissues

Our validated GC-MS/MS method for tissue SS measurements was then used to simultaneously map the SS pattern in serum and 10 different tissues from gonadal intact and ORX male mice: endocrine (testis, adrenals), reproductive (seminal vesicles, prostate, m. levator ani), tissues representative of the major body compartments (WAT, muscle, bone, brain), and liver.

Testosterone

In gonadal intact males, the highest concentration of T was found in the testis and high T levels were also found in WAT (Fig. 2A). A substantial part (60%) of the total body T pool was found in adipose tissue. The estimated total body pool of T decreased by as much as 99.7% after orchiectomy. T levels were reduced in all tissues except in the adrenals and liver, resulting in undetectable levels in most tissues. The remaining pool of T in ORX mice was mainly found in serum and the brain (Fig. 2B).

Dihydrotestosterone

In gonadal intact males, high DHT levels were, as expected, found in the endocrine and reproductive tissues, but remarkably, high DHT levels, similar to the levels in the testis, adrenals and prostate, were also found in WAT (Fig. 3A). The majority (88%) of the total body DHT pool was found in adipose tissue (Fig. 3B). The ratio of DHT to T, an indicator of local conversion of T to DHT or 5α-reductase activity, was

substantially higher than in serum in the seminal vesicles, prostate and adrenals, while it was moderately higher than in serum in m. levator ani and adipose tissue, suggesting there is local production of DHT from T in those tissues in gonadal intact male mice (Fig. 4). The total body pool of DHT decreased by 99.7% after orchiectomy. DHT levels were reduced in all tissues except the liver, resulting in undetectable levels in some but not all tissues. The remaining pool of DHT in ORX mice was mainly found in adipose tissue, liver, and the brain (Fig. 3B).

Table 6. Accuracy in mouse cortical bone

	Baseline	Spiked	Measured	Accuracy
	pg/g	pg/g	pg/g	(%)
Estradiol				
Low	0.0	2.0	2.4	119
High	0.0	10.0	9.4	94
Estrone				
Low	0.0	2.0	1.7	83
High	0.0	10.0	9.4	94
Testosterone				
Low	0.0	20.0	21.8	109
High	0.0	100	103	102
Dihydrotestosterone				
Low	0.0	8.0	9.5	119
High	0.0	20.0	22.4	112
Progesterone				
Low	0.0	75.0	76.5	102
High	0.0	375	370	99
Androstenedione				
Low	0.0	7.5	7.4	99
High	0.0	37.5	37.8	101

Accuracy was calculated as (measured level—baseline level)/ spiked level × 100%. Sample size 125 mg.

Androstenedione

In gonadal intact males, the highest concentration of the androgen precursor A-dione was found in the testis, with high A-dione levels also found in the adrenals and WAT (Fig. 5A). The adipose tissue (54%) and the testis (41%) were the major contributors to the total body pool of A-dione in gonadal intact mice. The total body pool of A-dione decreased by 96.5% after orchiectomy (Fig. 5B). The A-dione levels decreased in WAT, prostate and m. levator ani and increased in the seminal vesicles after orchiectomy (Fig. 5A).

Progesterone

In gonadal intact males, the highest concentration of Prog was found in the adrenals, with high Prog levels also observed in WAT (Fig. 6A). A substantial part (67%) of the total body Prog pool was found in adipose tissue (Fig. 6B). In contrast to the total body androgen pools, the total body pool of Prog increased after orchiectomy. Prog levels were increased in many tissues including all evaluated male reproductive tissues, as well as in adrenals, liver, and WAT. The total body pool of Prog in ORX mice was still mainly found in adipose tissue (75%) and the adrenals (11%; Fig. 6B).

Estradiol and estrone

E2 and E1 levels were only detectable in the testis (45 [43-49] pg/g and 2.3 [2.0-2.5] pg/g, respectively, median [IQR]).

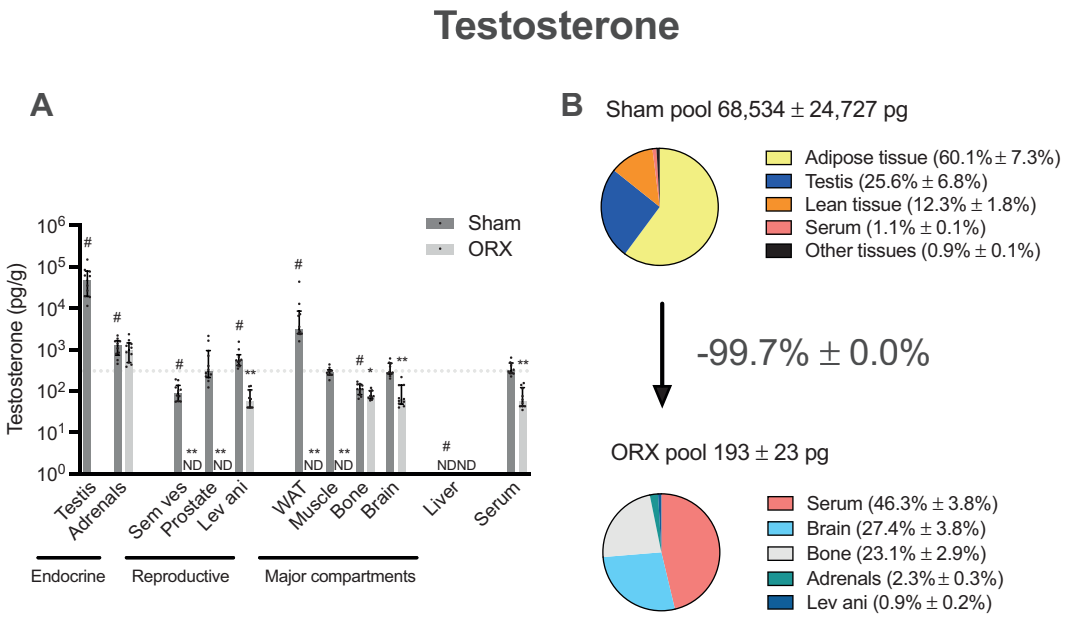

Figure 2. Testosterone (T) distribution in gonadal intact (Sham) and orchiectomized (ORX) young adult C57BL/6 male mice. (A) T concentrations in tissues and serum of Sham and ORX mice. Bars and error bars represent median ± IQR. N = 9-10/group. ND, not detected; WAT, white adipose tissue; Sem ves, seminal vesicles; Lev ani, m. levator ani. #Significant difference between tissue and serum T values in intact males ($P < .05$, Wilcoxon signed rank test, corrected for 10 multiple comparisons using the Holm–Sidak method). Differences between T concentrations in ORX and Sham mice were analyzed with Mann–Whitney U-test (*$P < .05$; **$P < .001$). (B) The relative calculated amounts of T in different tissues of Sham and ORX mice using a simplified whole-body model. Values are presented as mean ± SEM.

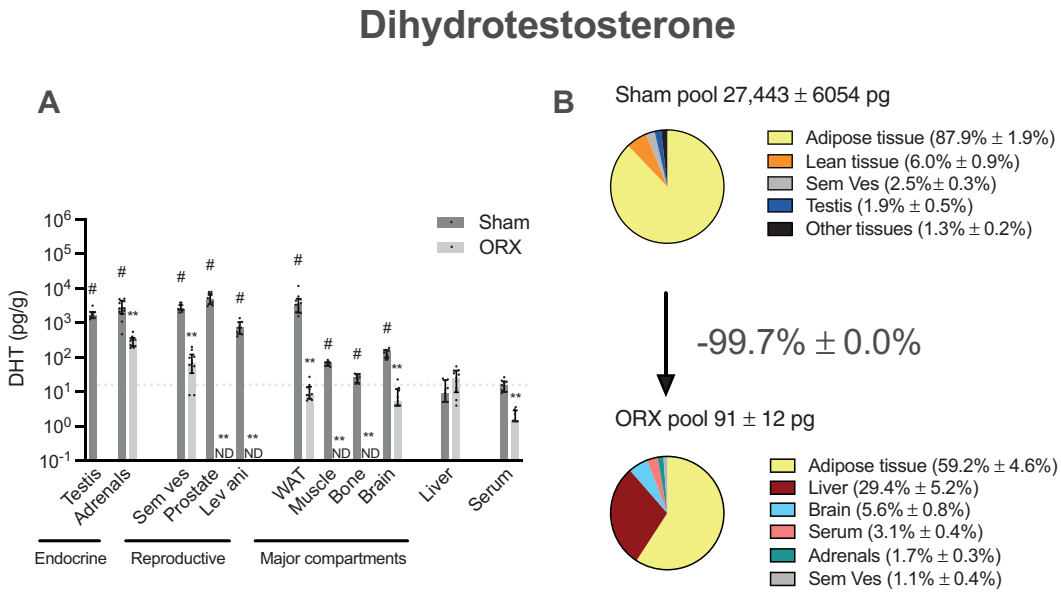

Figure 3. Dihydrotestosterone (DHT) distribution in gonadal intact (Sham) and orchiectomized (ORX) young adult C57BL/6 male mice. (A) DHT concentrations in tissues and serum of Sham and ORX mice. Bars and error bars represent median ± IQR. N = 9-10/group. ND = not detected, WAT, white adipose tissue; Sem ves, seminal vesicles; Lev ani, m. levator ani. #Significant difference between tissue and serum DHT values in intact males ($P < .05$, Wilcoxon signed rank test, corrected for 10 multiple comparisons using the Holm–Sidak method). Differences between DHT concentrations in ORX and Sham mice were analyzed with Mann–Whitney U-test (*$P < .05$; **$P < .001$). (B) The relative calculated amounts of DHT in different tissues of Sham and ORX mice using a simplified whole-body model. Values are presented as mean ± SEM.

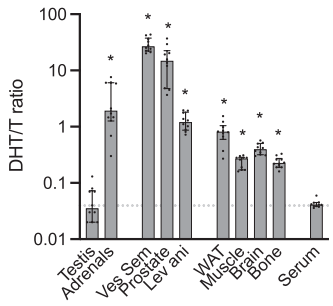

Figure 4. DHT/T ratio in different tissues of young adult gonadal intact C57BL/6 male mice. Bars and error bars represent median ± IQR. *Significant difference between tissue and serum DHT/T ratios ($P < .05$, Wilcoxon signed rank test, corrected for 10 multiple comparisons using the Holm–Sidak method). DHT, dihydrotestosterone; T, testosterone; WAT, white adipose tissue; Ves sem, seminal vesicles; Lev ani, m. levator ani.

Total Pool of SSs in Gonadal Intact and ORX Male Mice

In gonadal intact mice, the estimated total body pools of T, DHT, A-dione, and Prog were in the same range but with slightly larger pools of T and Prog compared with DHT and A-dione. After orchiectomy, the amounts of T, DHT, and A-dione decreased markedly whereas the Prog pool was approximately 1000-fold larger than the T and DHT pools and 100-fold larger than the A-dione pool (Fig. 7). Thus, Prog was by far the most abundant SSs in ORX mice.

SS Profiles of the Different Tissues

Next, we evaluated the SS profiles in each tissue, displaying varying patterns of SS levels in gonadal intact and ORX mice. In the testes of intact males, the highest SS concentrations were observed for T and A-dione (Fig. 8A). In the adrenals, Prog was the by far most abundant SSs both in gonadal intact and ORX mice (Fig. 8B). In the reproductive tissues, DHT was the most abundant SS in gonadal intact mice while Prog was the most abundant SS in ORX mice (Fig. 8C-8E). In WAT, the levels of T, DHT, A-dione, and Prog were within the same range in gonadal intact mice. However, after orchiectomy, the levels of T, DHT, and A-dione decreased markedly, whereas the Prog levels were more than 1000-fold higher than the T and DHT levels (Fig. 8F). In muscle, T and Prog were the most abundant SSs in gonadal intact mice. After orchiectomy, no detectable levels of T and DHT were observed, whereas the levels of Prog did not change (Fig. 8G). In cortical bone, T and Prog were the most abundant SSs in gonadal intact mice. Although DHT and T levels were reduced by orchiectomy, no substantial reductions of Prog levels were observed (Fig. 8H). In the brain cortex, T, DHT, and Prog were the most abundant SSs in gonadal intact mice, and after orchiectomy, T and DHT levels, but not Prog levels, were reduced (Fig. 8I). In the liver, the main SS-metabolizing organ, SS levels were overall low in intact mice. After orchiectomy, increased Prog levels and decreased A-dione levels were observed (Fig. 8J).

Correlations Between Circulating and Tissue Levels of SS

Using the fact that we have measured concentrations of SSs in serum and 10 different tissues of the same animals, we next explored the correlations between circulating and tissue levels of SSs in gonadal intact (Table 7) and ORX mice (Table 8). In gonadal intact mice, circulating levels of DHT, T, and Prog were strongly correlated with corresponding levels in the brain while only modest correlations with corresponding levels in WAT and in the SS-producing testis and adrenals were observed. Serum levels of T and Prog showed strong correlations with their respective muscle levels (Table 7). In ORX mice, serum Prog levels were strongly correlated with Prog levels in multiple tissues, including m. levator ani, WAT, muscle,

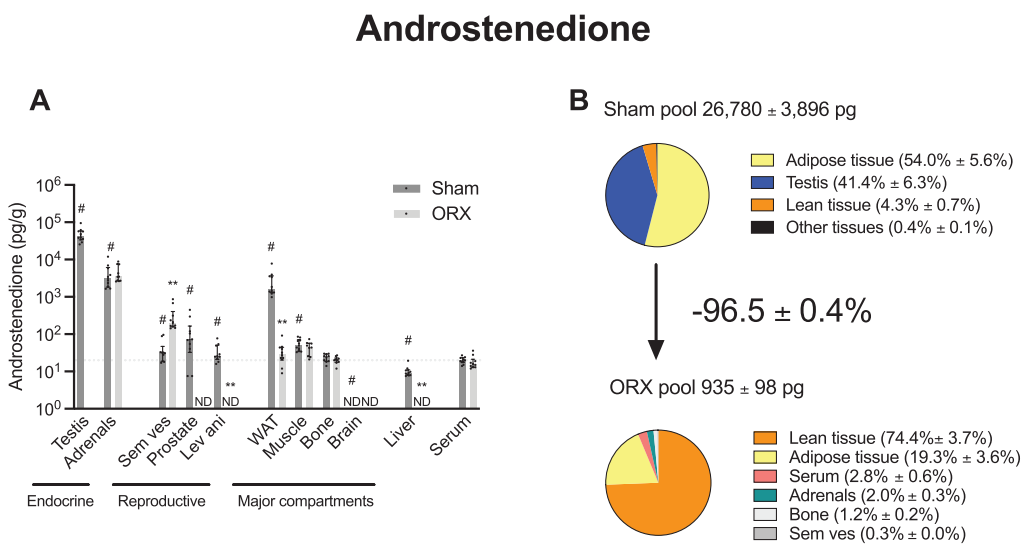

Figure 5. Androstenedione (A-dione) distribution in gonadal intact (Sham) and orchiectomized (ORX) young adult C57BL/6 male mice. (A) A-dione concentrations in tissues and serum of Sham and ORX mice. Bars and error bars represent median ± IQR. N = 9-10/group. ND, not detected; WAT, white adipose tissue; Sem ves, seminal vesicles; Lev ani, m. levator ani. #Significant difference between tissue and serum A-dione values in intact males ($P < .05$, Wilcoxon signed rank test, corrected for 10 multiple comparisons using the Holm–Sidak method). Differences between A-dione concentrations in ORX and Sham mice were analyzed with Mann–Whitney U-test (*$P < .05$; **$P < .001$). (B) The relative calculated amounts of A-dione in different tissues of Sham and ORX mice using a simplified whole-body model. Values are presented as mean ± SEM.

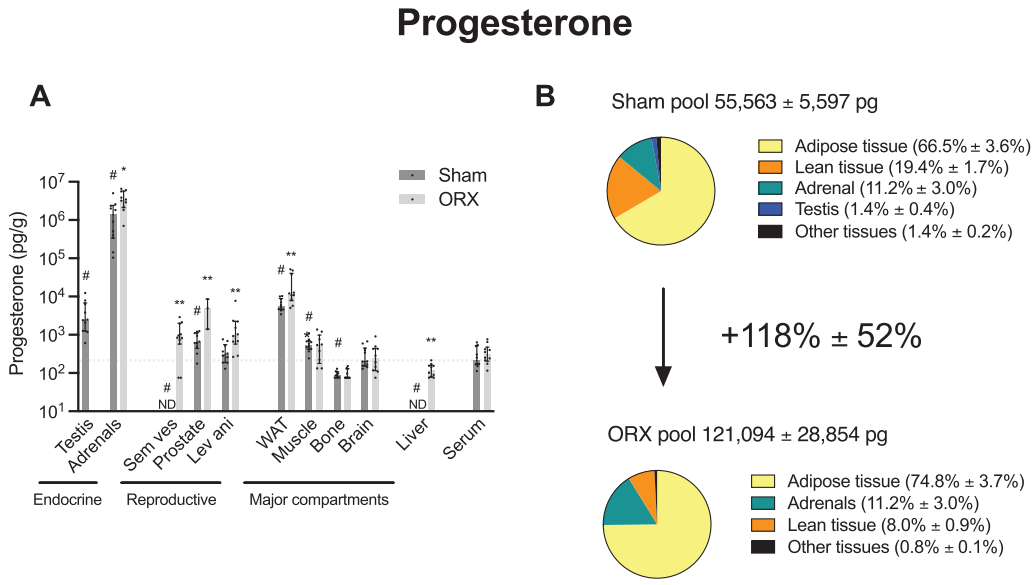

Figure 6. Progesterone (Prog) distribution in gonadal intact (Sham) and orchiectomized (ORX) young adult C57BL/6 male mice. (A) Prog concentrations in tissues and serum of Sham and ORX mice. Bars and error bars represent median ± IQR. N = 9-10/group. ND, not detected; WAT, white adipose tissue; Sem ves, seminal vesicles; Lev ani, m. levator ani. #Significant difference between tissue and serum Prog values in intact males ($P < .05$, Wilcoxon signed rank test, corrected for 10 multiple comparisons using the Holm-Sidak method). Differences between Prog concentrations in ORX and Sham mice were analyzed with Mann–Whitney U-test (*$P < .05$; **$P < .001$). (B) The relative calculated amounts of Prog in different tissues of Sham and ORX mice using a simplified whole-body model. Values are presented as mean ± SEM.

bone, and brain cortex (Table 8). Further explorative correlation analyses for Prog, the most abundant SS in serum of ORX mice, revealed that serum Prog levels were significantly correlated with serum DHT levels in ORX mice ($r_s = 0.71$, $P = .02$) but not in gonadal intact mice ($r_s = 0.39$, $P = .26$). Serum Prog levels were also associated with DHT levels in the brain ($r_s = 0.68$, $P = .03$) in ORX mice. In addition, serum DHT levels were strongly correlated with levels of brain DHT in ORX mice (Table 8). Evaluation of correlations within the brain cortex revealed that DHT and T concentrations were significantly correlated in gonadal intact ($r_s = 0.71$, $P = .022$) but not in ORX mice ($r_s = 0.49$, $P = .16$). In contrast, DHT levels in the brain cortex correlated significantly with brain Prog in ORX mice ($r_s = 0.68$, $P = .031$). Thus, in gonadal intact mice, there is a strong correlation between brain concentrations of T and DHT. In contrast, in ORX mice, serum and brain Prog levels but not brain T levels are correlated with brain DHT levels.

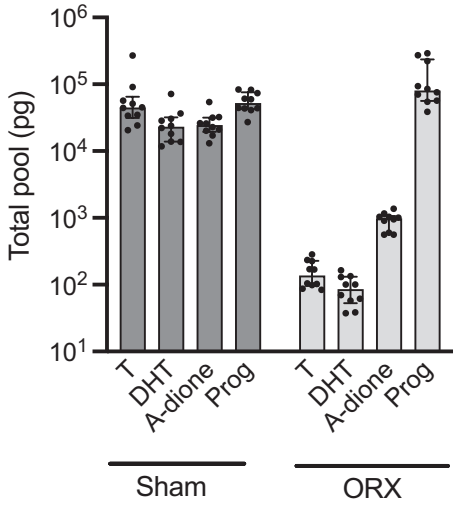

Figure 7. Total pool of sex steroids in gonadal intact (Sham) and orchiectomized (ORX) young adult C57BL/6 male mice using a simplified whole-body model. Bars and error bars represent median ± IQR. N = 9-10/group. T, testosterone; DHT, dihydrotestosterone; A-dione, androstenedione; Prog, progesterone.

Discussion

Local metabolism of SSs is generally believed to be crucial for SS action, but a comprehensive atlas of SS distribution in multiple tissues is still lacking. In addition, it remains largely unknown to what extent circulating levels of SSs correlate with tissue levels of SSs. We here developed and validated a highly sensitive GC-MS/MS method with excellent sensitivity, precision, and accuracy for measurement of a broad panel of SSs in several different types of mouse tissues. Using this assay, we present a comprehensive atlas of tissue and serum concentrations of SSs in gonadal intact and ORX male mice. Our findings in gonadal intact mice indicate that the brain androgen and Prog levels are well reflected by the circulating levels of the corresponding SSs and that WAT constitutes a large reservoir of SSs. In addition, Prog is by far the most abundant SS after orchiectomy and correlates with circulating and brain DHT levels.

SSs receptors and enzymes involved in SS metabolism are present in brain tissue, and local SS synthesis has been thoroughly described (5). Several previous studies described measurable levels of Prog, T, and DHT in different brain regions of rodents (20, 25-28). However, to the best of our knowledge, no previous study evaluated the correlations between SS levels, measured using validated and specific MS-based methods, in the circulation and in the brain of male rodents. We found strong correlations between serum and cortical brain concentrations of T, DHT, and Prog in gonadal intact male mice. This finding confirms that lipophilic SSs easily pass the blood–brain barrier (29). This may suggest that in mice, which lack SHBG in the circulation (10), the levels of T, DHT, and Prog in the central nervous system are well reflected by their corresponding levels in the circulation. However, it should be emphasized that in humans, a substantial part of SS circulates tightly bound to SHBG and, therefore, the correlation between circulating SS levels and SS levels in the brain might be weaker in men than the associations observed in the male mice in this study. A recent study failed to identify any significant association between T levels in serum and the cerebrospinal fluid in healthy men (30) but it is possible that the study results were affected by the fact that an immunoassay-based technique was used for the SS analyses and not a gold standard MS-based technique.

Adipose tissue is a known site of androgen action (31) and has been described as an endocrine organ with the ability to locally produce and metabolize several SSs (32, 33). We observed high DHT levels in WAT and the majority of the total body reservoir of androgens (T and DHT) and Prog was found in WAT in gonadal intact male mice. The ratio of DHT to T was clearly higher in WAT than in serum, suggesting that some local production of DHT from T occurs in adipose tissue, which is in agreement with the reported expression of *Srd5a1* in male mouse gonadal fat tissue (34, 35). In addition, the correlations between SS levels in serum and WAT were modest, indicating that the high SS concentrations in adipose tissue are partly independently regulated compared with the substantially lower concentrations observed in the circulation. In humans, SHBG has an important role as a buffer of circulating SS concentrations. It is unknown how mice, lacking the buffer action of SHBG (10), are protected from extreme SS fluctuations. As SSs are lipophilic and the largest reservoir of androgens in the mouse body is found in WAT, we propose that WAT may act as a functional buffer for circulating SS levels in male mice. In situations with very high circulating androgen levels, androgens may leave the circulation and be stored in WAT while in situations with very low circulating androgens, WAT-derived androgens may be released to the circulation. However, further functional studies are warranted to verify this hypothesis.

In the present study, orchiectomy predictably decreased T and DHT levels in the circulation and multiple tissues while Prog levels in male reproductive tissues, adrenals, and WAT increased. Our findings suggest that Prog levels may be slightly upregulated in some tissues as a response to the removal of testicular androgens. The role of Prog in male physiology is still not fully characterized (36, 37). Administration of Prog to male rats stimulated prostate growth, partly by androgenic products and partly through the Prog receptor (38). Also, 17-hydroxyProg can be metabolized into the potent androgen DHT both via the classic pathway and the alternative "backdoor" pathway (4). Although androgen levels in the present study in general decreased substantially after orchiectomy, some organs still contained measurable levels, supporting previous studies that other sources of androgens than the testis are available in male mice (18). Even though mouse adrenals do not produce large amounts of dehydroepiandrosterone, they may contribute to the androgen pool in ORX mice by producing other androgen precursors (18, 23). Indeed, Huhtaniemi et al. showed upregulation of *Cyp17a1* expression in the mouse adrenal after orchiectomy, enabling measurable androgen production from Prog (23). After orchiectomy, Prog was the most abundant SS in serum and multiple tissues and WAT constituted the major reservoir of Prog in the mouse body. The high levels of Prog in ORX mice demonstrate that Prog is not testis derived while the very high Prog levels in the adrenals support the notion that the adrenals contribute to the large Prog pool in ORX mice. A possible follow-up experiment to decipher the source of the remaining SSs present after orchiectomy would be to perform orchiectomy and adrenalectomy simultaneously. The estimated total body Prog pool was more than 1000-fold higher than the total body T and DHT pools in ORX male mice. We observed that Prog levels in WAT and serum correlated significantly in

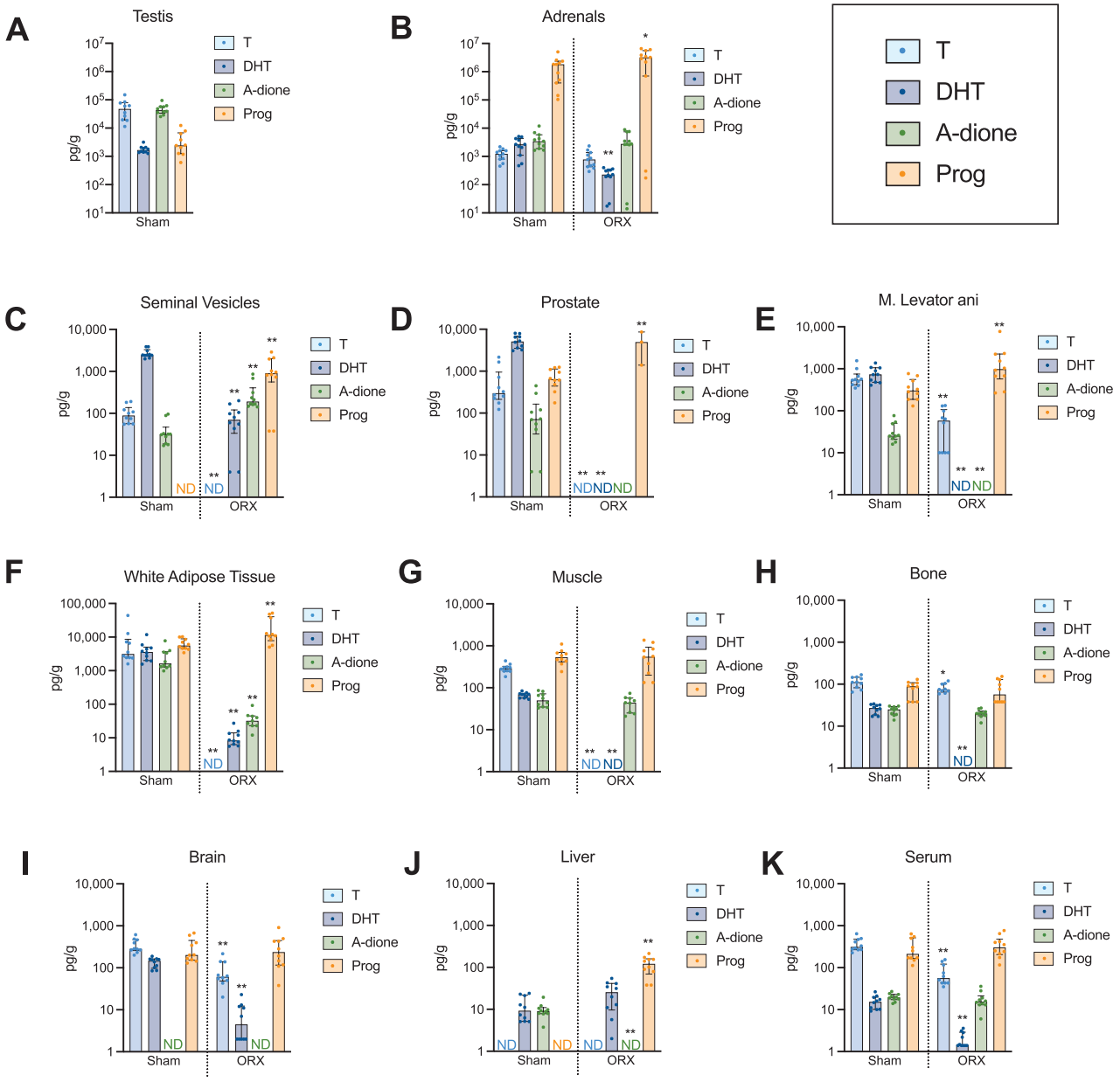

Figure 8. Sex steroid profiles in tissues and serum of gonadal intact (Sham) and orchiectomized (ORX) young adult male C57BL/6 mice. Bars and error bars represent median ± IQR. N = 9-10/group (except for prostate ORX, n = 3). T, testosterone; DHT, dihydrotestosterone; A-dione, androstenedione; Prog, progesterone. Stars represent statistically significant difference compared to the corresponding hormone in Sham. Mann-Whitney U-test (* $P <$ .05, ** $P <$ .001).

Table 7. Correlations between serum and tissue sex steroid levels in gonadal intact male mice

	Tissue									
	Endocrine		Reproductive			Major body compartments				
Serum	Testis	Adrenals	SV	Prostate	LA	WAT	Muscle	Bone	Brain	Liver
Testosterone	0.30	0.36	**0.83**	0.54	**0.77**	0.61	**0.82**	0.54	**0.93**	NA
DHT	0.03	–0.36	0.55	**0.77**	0.22	0.31	0.09	0.41	**0.86**	**0.76**
A-dione	–0.21	–0.16	0.10	0.61	0.41	**0.87**	0.22	0.38	NA	0.56
Progesterone	0.26	**0.65**	NA	0.30	**0.66**	0.25	**0.84**	**0.79**	**0.94**	NA

Spearman correlations are given. Bold indicates $P <$ .05, N = 9-10.
Abbreviations: A-dione, androstenedione; DHT, dihydrotestosterone; LA, m. levator ani; NA, not available; SV, seminal vesicles, WAT, white adipose tissue.

Table 8. Correlations between serum and tissue sex steroid levels in orchiectomized male mice

	Tissue									
	Endocrine		Reproductive			Major body compartments				
Serum	Testis	Adrenals	SV	Prostate	LA	WAT	Muscle	Bone	Brain	Liver
Testosterone	NA	0.19	NA	NA	0.20	NA	NA	0.07	0.23	NA
DHT	NA	–0.03	0.08	NA	NA	**0.67**	NA	NA	**0.93**	0.34
A-dione	NA	0.36	–0.21	NA	NA	–0.19	–0.37	0.37	NA	NA
Progesterone	NA	0.49	0.58	NA	**0.88**	**0.84**	**0.87**	**0.90**	**0.95**	0.44

Spearman correlations are given. Bold indicates $P < .05$, N = 9-10.
Abbreviations: A-dione, androstenedione; DHT, dihydrotestosterone; LA, m. levator ani; NA, not available; SV, seminal vesicles, WAT, white adipose tissue.

ORX mice. Serum Prog levels, in turn, correlated with serum DHT levels and brain DHT levels in ORX mice. These observational associations may suggest that the large pool of Prog contributes to DHT in the circulation and the brain in ORX mice. While Prog is an abundant hormone in male mice and humans, its physiological role and origin are surprisingly understudied. Thus, functional studies are warranted to determine the possible roles of Prog, acting either directly via the Prog receptor or indirectly via downstream tissue-specific metabolism to active androgens (Fig. 1), in ORX mice.

Even though tissue weights of androgen-responsive organs have been used as indicators of androgen exposure, their local steroid milieus are still largely unknown. Interestingly, in m. levator ani, A-dione was absent after orchiectomy while T was present, suggesting a short half-life of A-dione locally by rapid metabolism to T or other downstream metabolites. Furthermore, there was an increased concentration of A-dione in the seminal vesicles after orchiectomy, suggesting the possibility for local Cyp17a1 induction by orchiectomy, to be addressed in future experiments.

A major strength of the present study is the development and use of a validated gold standard MS-based method for SS measurements as the commonly used immunoassay-based techniques have a questionable specificity, especially in the lower concentration range (12, 14, 39-42). Another strength is that this study is the first to simultaneously determine a broad panel of SSs both in the circulation and in multiple tissues, allowing the evaluation of correlations between circulating SS levels and corresponding intra-tissue levels. Our findings demonstrate that the strengths of the correlations between circulating SS levels and corresponding tissue SS levels differ substantially between tissues and evaluated SSs and depend on the presence of testis-derived SSs. This information is valuable for researchers to determine if easily accessible circulating SS levels can be used as relevant proxies for tissue levels of SSs in male mice. The present study is the first to estimate the whole-body pool of SSs in gonadal intact and ORX mice. However, it should be emphasized that we used a simplified model that could be further refined by measurement of SSs in additional tissues. Mouse prostates express several steroid-metabolizing enzymes (43). A technical limitation of this study is that prostate samples were only available from 3 ORX mice, and sample sizes were small due to the expected decrease in prostate size after orchiectomy. As the whole prostate is used for the SS analyses, the reduced prostate weight in ORX mice resulted in substantially reduced sensitivity of our assay to detect possible remaining androgens. Finally, although it is well known that estrogen actions mediated via estrogen receptors in multiple tissues are crucial for male mouse physiology (44), we did not detect E2 or E1 levels in serum or tissues of male mice except in the testes using our gold standard method with LLOQ around 2 pg/g in tissues. Further developments of MS-based methods with a magnitude of improvement in sensitivity for E2 and E1 are most likely required for reliable analyses of estrogen levels in male mice.

In this study, we have validated a novel, highly sensitive analysis method and explored local levels of SSs in several tissue types in mice, creating a tissue atlas of the steroid pool in male mice with and without orchiectomy. Further studies are needed to examine the correlations between local steroid levels and SS-metabolizing enzymes in tissues. Such future studies will deepen our understanding of local steroid production and metabolism in peripheral tissues in mice and provide further insight into the translatability of the endocrinology of rodents to humans.

In conclusion, we here present a comprehensive atlas of tissue and serum concentrations of SSs in male mice revealing novel insights in SS distribution. We demonstrate that the brain SS levels are well reflected by serum levels of SSs in male mice. In addition, WAT constitutes a large reservoir of SSs, and we propose that it may act as a buffer for circulating SS levels in male mice. Finally, Prog is by far the most abundant SS in ORX mice and further studies should determine the role of Prog in male mice lacking testicular androgens.

Acknowledgments

The authors thank Biljana Aleksic and Lotta Uggla for excellent technical assistance.

Funding

This study was supported by the Swedish Research Council, Vetenskapsrådet (grant numbers: 2019-01295 (SHW), 2018-02600 (LV), 2016-01001 (CO)) and by grant from the Swedish state under the agreement between the Swedish government and the county councils (the ALF-agreement), the IngaBritt and Arne Lundberg Foundation (grant number 2017-0081), the Torsten Söderberg Foundation (grant numbers: M65/15, MT3/20), the Novo Nordisk Foundation (NNF180C0033898), and the Knut and Alice Wallenberg Foundation (grant numbers: KAW2015.0317, 2020.0230).

Author Contributions

Author roles: Designed research: M.N., M.P., H.R., L.V., C.O. Performed research: M.N., A.K.N., A.L., S.H.W., J.W., K.L.G., L.V. Analyzed data: H.C., A.K.N., A.L., H.R., M.P.,

L.V., C.O. Wrote the manuscript: H.C., L.V., C.O. Revised the manuscript: H.C., M.N., A.K.N., A.L., S.H.W., J.W., K.L.G., M.P., H.R. L.V., C.O. All authors approved the final version of the manuscript. H.C. and C.O. take responsibility for the integrity of the data analysis.

Disclosure Summary

The authors state that they have no conflicting interests.

Data Availability

The datasets generated and analyzed during the current study are not publicly available but are available from the corresponding author on reasonable request.

References

1. Labrie F, Luu-The V, Labrie C, *et al*. Endocrine and intracrine sources of androgens in women: inhibition of breast cancer and other roles of androgens and their precursor dehydroepiandrosterone. *Endocr Rev*. 2003;24(2):152-182.
2. Schiffer L, Arlt W, Storbeck KH. Intracrine androgen biosynthesis, metabolism and action revisited. *Mol Cell Endocrinol*. 2018;465:4-26.
3. Heinosalo T, Saarinen N, Poutanen M. Role of hydroxysteroid (17beta) dehydrogenase type 1 in reproductive tissues and hormone-dependent diseases. *Mol Cell Endocrinol*. 2019;489:9-31.
4. O'Shaughnessy PJ, Antignac JP, Le Bizec B, *et al*. Alternative (backdoor) androgen production and masculinization in the human fetus. *PLoS Biol*. 2019;17(2):e3000002.
5. Fokidis HB, Adomat HH, Kharmate G, Hosseini-Beheshti E, Guns ES, Soma KK. Regulation of local steroidogenesis in the brain and in prostate cancer: lessons learned from interdisciplinary collaboration. *Front Neuroendocrinol*. 2015;36:108-129.
6. Schmidt KL, Pradhan DS, Shah AH, Charlier TD, Chin EH, Soma KK. Neurosteroids, immunosteroids, and the Balkanization of endocrinology. *Gen Comp Endocrinol*. 2008;157(3):266-274.
7. Duarte AC, Hrynchak MV, Gonçalves I, Quintela T, Santos CR. Sex hormone decline and amyloid β synthesis, transport and clearance in the brain. *J Neuroendocrinol*. 2016;28(11):1–22.
8. Penning TM, Detlefsen AJ. Intracrinology-revisited and prostate cancer. *J Steroid Biochem Mol Biol*. 2020;196:105499.
9. Zhao H, Zhou L, Shangguan AJ, Bulun SE. Aromatase expression and regulation in breast and endometrial cancer. *J Mol Endocrinol*. 2016;57(1):R19-R33.
10. Jänne M, Deol HK, Power SG, Yee SP, Hammond GL. Human sex hormone-binding globulin gene expression in transgenic mice. *Mol Endocrinol*. 1998;12(1):123-136.
11. McNamara KM, Harwood DT, Simanainen U, Walters KA, Jimenez M, Handelsman DJ. Measurement of sex steroids in murine blood and reproductive tissues by liquid chromatography-tandem mass spectrometry. *J Steroid Biochem Mol Biol*. 2010;121(3-5):611-618.
12. Nilsson ME, Vandenput L, Tivesten A, *et al*. Measurement of a comprehensive sex steroid profile in rodent serum by high-sensitive gas chromatography-tandem mass spectrometry. *Endocrinology*. 2015;156(7):2492-2502.
13. Handelsman DJ, Gibson E, Davis S, Golebiowski B, Walters KA, Desai R. Ultrasensitive serum Estradiol measurement by liquid chromatography-mass spectrometry in postmenopausal women and mice. *J Endocr Soc*. 2020;4(9):bvaa086.
14. Rosner W, Hankinson SE, Sluss PM, Vesper HW, Wierman ME. Challenges to the measurement of estradiol: an endocrine society position statement. *J Clin Endocrinol Metab*. 2013;98(4):1376-1387.
15. Demers LM. Testosterone and estradiol assays: current and future trends. *Steroids*. 2008;73(13):1333-1338.
16. Knuuttila M, Hämäläinen E, Poutanen M. Applying mass spectrometric methods to study androgen biosynthesis and metabolism in prostate cancer. *J Mol Endocrinol*. 2019;62(4):R255-R267.
17. Weng Y, Xie F, Xu L, Zagorevski D, Spink DC, Ding X. Analysis of testosterone and dihydrotestosterone in mouse tissues by liquid chromatography–electrospray ionization–tandem mass spectrometry. *Anal Biochem*. 2010;402(2):121-128.
18. Mostaghel EA, Zhang A, Hernandez S, *et al*. Contribution of adrenal glands to intratumor androgens and growth of castration-resistant prostate cancer. *Clin Cancer Res*. 2019;25(1):426-439.
19. Tobiansky DJ, Korol AM, Ma C, *et al*. Testosterone and corticosterone in the mesocorticolimbic system of male rats: effects of gonadectomy and caloric restriction. *Endocrinology*. 2018;159(1):450-464.
20. Caruso D, Pesaresi M, Maschi O, Giatti S, Garcia-Segura LM, Melcangi RC. Effect of short-and long-term gonadectomy on neuroactive steroid levels in the central and peripheral nervous system of male and female rats. *J Neuroendocrinol*. 2010;22(11):1137-1147.
21. Hennig K, Antignac JP, Bichon E, *et al*. Steroid hormone profiling in human breast adipose tissue using semi-automated purification and highly sensitive determination of estrogens by GC-APCI-MS/MS. *Anal Bioanal Chem*. 2018;410(1):259-275.
22. Collden H, Landin A, Wallenius V, *et al*. The gut microbiota is a major regulator of androgen metabolism in intestinal contents. *Am J Physiol Endocrinol Metab*. 2019;317(6):E1182-E1192.
23. Huhtaniemi R, Oksala R, Knuuttila M, *et al*. Adrenals contribute to growth of castration-resistant VCaP prostate cancer xenografts. *Am J Pathol*. 2018;188(12):2890-2901.
24. Colldén H, Nilsson ME, Norlén A-K, *et al*. Data from: Supplementary figures from Comprehensive sex steroid profiling in multiple tissues reveals novel insights in sex steroid distribution in gonadal intact and orchiectomized male mice. Zenodo. Deposited December 23. Doi: 10.5281/zenodo.5786536
25. Hamden JE, Gray KM, Salehzadeh M, *et al*. Steroid profiling of glucocorticoids in microdissected mouse brain across development. *Dev Neurobiol*. 2021;81(2):189-206.
26. Caruso D, Pesaresi M, Abbiati F, *et al*. Comparison of plasma and cerebrospinal fluid levels of neuroactive steroids with their brain, spinal cord and peripheral nerve levels in male and female rats. *Psychoneuroendocrinology*. 2013;38(10):2278-2290.
27. Li J, Gibbs RB. Detection of estradiol in rat brain tissues: contribution of local versus systemic production. *Psychoneuroendocrinology*. 2019;102:84-94.
28. Teubel J, Parr MK. Determination of neurosteroids in human cerebrospinal fluid in the 21st century: a review. *J Steroid Biochem Mol Biol*. 2020;204:105753.
29. Banks WA. Brain meets body: the blood-brain barrier as an endocrine interface. *Endocrinology*. 2012;153(9):4111-4119.
30. Martin J, Plank E, Jungwirth B, Hapfelmeier A, Podtschaske A, Kagerbauer SM. Weak correlations between serum and cerebrospinal fluid levels of estradiol, progesterone and testosterone in males. *BMC Neurosci*. 2019;20(1):53.
31. O'Reilly MW, House PJ, Tomlinson JW. Understanding androgen action in adipose tissue. *J Steroid Biochem Mol Biol*. 2014;143:277-284.
32. Bélanger C, Luu-The V, Dupont P, Tchernof A. Adipose tissue intracrinology: potential importance of local androgen/estrogen metabolism in the regulation of adiposity. *Horm Metab Res*. 2002;34(11-12):737-745.
33. Kinoshita T, Honma S, Shibata Y, *et al*. An innovative LC-MS/MS-based method for determining CYP 17 and CYP 19 activity in the adipose tissue of pre- and postmenopausal and ovariectomized women using 13C-labeled steroid substrates. *J Clin Endocrinol Metab*. 2014;99(4):1339-1347.
34. Mouse Genome Database (MGD). The Jackson Laboratory, Bar Harbor, Maine. Accessed December 2021. http://www.informatics.jax.org
35. Molaie S, Shahverdi A, Sharafi M, *et al*. Dietary trans and saturated fatty acids effects on semen quality, hormonal levels and expression

of genes related to steroid metabolism in mouse adipose tissue. *Andrologia*. 2019;51(5):e13259.
36. Oettel M, Mukhopadhyay AK. Progesterone: the forgotten hormone in men? *Aging Male*. 2004;7(3):236-257.
37. Grindstad T, Richardsen E, Andersen S, *et al*. Progesterone receptors in prostate cancer: progesterone receptor B is the isoform associated with disease progression. *Sci Rep*. 2018;8(1):11358.
38. Nishino T, Ishibashi K, Hirtreiter C, Nishino Y. The prostate growth stimulation by progesterone is due to androgenic products and progesterone receptor-mediated mechanisms. *Pharmazie*. 2009;64(9):587-589.
39. Lee JS, Ettinger B, Stanczyk FZ, *et al*. Comparison of methods to measure low serum estradiol levels in postmenopausal women. *J Clin Endocrinol Metab*. 2006;91(10):3791-3797.
40. Haisenleder DJ, Schoenfelder AH, Marcinko ES, Geddis LM, Marshall JC. Estimation of estradiol in mouse serum samples: evaluation of commercial estradiol immunoassays. *Endocrinology*. 2011;152(11):4443-4447.
41. Huhtaniemi IT, Tajar A, Lee DM, *et al*. Comparison of serum testosterone and estradiol measurements in 3174 European men using platform immunoassay and mass spectrometry; relevance for the diagnostics in aging men. *Eur J Endocrinol*. 2012;166(6):983-991.
42. Ohlsson C, Nilsson ME, Tivesten A, *et al*. Comparisons of immunoassay and mass spectrometry measurements of serum estradiol levels and their influence on clinical association studies in men. *J Clin Endocrinol Metab*. 2013;98(6):E1097-E1102.
43. Pelletier G, Luu-The V, Li S, Ouellet J, Labrie F. Cellular localization of mRNA expression of enzymes involved in the formation and inactivation of hormonal steroids in the mouse prostate. *J Histochem Cytochem*. 2004;52(10):1351-1356.
44. Vanderschueren D, Laurent MR, Claessens F, *et al*. Sex steroid actions in male bone. *Endocr Rev*. 2014;35(6):906-960.